Quiles-Carrillo, L.; Duart, S.; Montanes, N.; Torres-Giner, S.; Balart, R. (2018). Enhancement of the mechanical and thermal properties of injection-molded polylactide parts by the addition of acrylated epoxidized soybean oil. Materials & Design. 140:54-63. https://doi.org/10.1016/j.matdes.2017.11.031

Enhancement of mechanical and thermal properties of injection-molded polylactide parts by addition of acrylated epoxidized soybean oil

L. Quiles-Carrillo[1], S. Duart[1], N. Montanes[1], S. Torres-Giner[2], and R. Balart[1,*]

[1] Technological Institute of Materials (ITM), Universitat Politècnica de València (UPV), Plaza Ferrándiz y Carbonell 1, 03801 Alcoy, Spain

[2] Novel Materials and Nanotechnology Group, Institute of Agrochemistry and Food Technology (IATA), Spanish Council for Scientific Research (CSIC), Calle Catedrático Agustín Escardino Benlloch 7, 46980 Paterna, Spain

***Corresponding author**:
PhD Rafael Antonio Balart Gimeno
Full Professor of Materials Science
Universitat Politècnica de València (UPV)
e-mail: rbalart@mcm.upv.es
Tel.: (+34) 96 652 84 21
Fax: (+34) 96 652 84 33

ABSTRACT

This work reports the effect of acrylated epoxidized soybean oil (AESO) addition on the mechanical, thermal, and thermomechanical properties of polylactide (PLA) parts obtained by injection molding. To this end, AESO, a chemically multi-functionalized vegetable oil, was incorporated into PLA during melt processing. The PLA parts with AESO contents in the 2.5–7.5 wt% range showed a remarkable enhancement in both elongation at break and impact-absorbed energy while their tensile and flexural strength as well as thermomechanical properties were maintained or slightly improved. Additionally, the AESO-containing PLA parts presented higher thermal stability and lower crystallinity. The improvement achieved was ascribed to a dual effect of plasticization in combination with a chain-extension and/or cross-linking process of the PLA chains by the highly reactive acrylate and epoxy groups present in AESO. The use of AESO thus represents an environmentally friendly solution to obtain toughened PLA materials of high interest in, for instance, rigid packaging, automotive or building and construction applications.

KEYWORDS: PLA; AESO; Mechanical properties; Thermal properties; Reactive extrusion; Injection molding

1. INTRODUCTION

Polylactide (PLA) is currently considered the front runner in the emerging bioplastics market due to its good balance between physical properties, *i.e.* mechanical, thermal, optical, and barrier properties, and its two-fold environmental advantage of being a bio-based and biodegradable material. For these reasons it is nowadays widely used in 3D printing, biomedical devices, rigid packaging, drug delivery systems, textiles, automotive parts, building and construction materials, etc.[1-5] The main drawbacks of PLA, however, are related to its intrinsic brittleness, which is a limiting factor to further expand its applications in commodity areas (*e.g.* packaging) [6, 7]. Today, with the increasing use of PLA as the base material for 3D printing and short-term uses [8, 9], the fragility of PLA is certainly an important issue to overcome [10-13]. For this reason, the vast majority of PLA industrial formulations are based on either plasticized formulations by means of additives or polymer blends [14-19].

A wide variety of plasticizers have been previously proposed for PLA. Different monomeric, oligomeric, and polymeric esters from adipic [20], citric [21-24], succinic [25], and lactic acid [26, 27], among others, have offered interesting results for PLA materials in terms of plasticization and/or compatibilization with other bio-based polyesters [28]. Another interesting family is that corresponding to polyhydric alcohols and their esters. Although glycerol is known to exert a poor plasticizing effect on PLA, both oligomeric and polymeric glycols and some related esters have been successfully used to plasticize PLA [29]. It is worthy to note the good plasticizing effect that poly(ethylene glycol) (PEG) [21, 30], poly(propylene glycol) (PPG) [31, 32], and their copolymers [33] can provide on PLA. Isosorbide esters have also been reported as good plasticizers for PLA and other polymers [34, 35]. Acrylic/acrylated oligomers and

polymers have also been reported to offer a good plasticizing effect on PLA in combination with a chain extension phenomenon, which improves toughness [36, 37].

With regard to vegetable oils, it is worthy to note their increasing use in the polymer industry as both the starting materials for polymer synthesis and additives [38-40]. Vegetable oils consist on a triglyceride structure in which different fatty acids are chemically bonded to a glycerol molecule through ester bonds. The main feature of some fatty acids is the presence of carbon–carbon double bonds that allows for a wide variety of chemical modifications. Unmodified vegetable oils have been used as PLA plasticizers but their performance is restricted due to the high difference in their solubility parameter (around 16 MPa $^{1/2}$) compared to that of PLA, in the 19.5–20.5 MPa $^{1/2}$ range [41, 42], which typically results in a migration process. For this reason, chemically modified vegetable oils offer a better plasticizing efficiency since their solubility parameters are closer to that of PLA [43].

In particular, the use of epoxidized vegetable oils (EVOs) represents an environmentally friendly solution to plasticize PLA and other polymers. As a result, several EVOs have been successfully used as PLA plasticizers. It is worthy to note the good plasticizing effect exerted by epoxidized fatty acid esters (EFAE) [44, 45], epoxidized soybean oil (ESBO) and palm oil [46, 47], and epoxidized linseed oil (ELO) [48]. The epoxy functionality present in EVOs also offers a high compatibilization on green composites with lignocellulosic fillers due to the reaction of the epoxide ring with the hydroxyl groups present in both PLA end-chains and cellulose [49]. This effect of compatibilization provided by EVOs has also been observed in vinyl plastisol/wood flour composites [50], thus emphasizing the extraordinary reactivity of the epoxy group.

Another interesting modification of vegetable oils is maleinization, which allows the formation of several maleic anhydride (MAH) groups, *i.e.* multiple functionalities,

from the different degrees of unsaturation originally present in the fatty acids. Maleinized vegetable oils such as maleinized linseed oil (MLO), maleinized cottonseed oil (MCSO), and maleinized tung oil (MTO) have been successfully used in toughened PLA formulations with an interesting combination of plasticization, chain-extension, and compatibilizing effects [51-54]. Acrylated epoxidized vegetable oils (AEVOs) are obtained by reaction of EVOs with acrylic acid (AA). Specifically, acrylated epoxidized soybean oil (AESO) has been reported as an environmentally friendly additive for toughening PLA-based blends [55].

Injection molding of PLA has to face some challenges related to its chemical structure [56]. Similar to other biopolyesters, PLA is particularly sensitive to moisture, which decreases its molecular weight (M_W) during processing [57], inducing a remarkable impairment on the mechanical performance. Additionally, its intrinsic brittleness also restricts a wider use of PLA materials in injection molding. In this sense, the injection molding industry uses different additives to control crystallization phenomena to improve mechanical properties [58, 59]. Another increasing trend within the injection-molded PLA context is related to use of green composites based on natural fibers [60, 61]. Finally, PLA blends also represent a relevant alternative for toughened-PLA formulations processed by injection molding but, usually, compatibilizers are needed [62].

Although several works have been previously focused on AESO-modified PLA films, the effect of AESO on PLA materials obtained by injection molding has not been evaluated. This work aims to carry out, for the first time, an in-depth study of the influence of AESO on the properties of injection-molded PLA parts. To this end, the effect of different AESO contents in the 2.5–10 wt% range were evaluated on the performance of the PLA parts.

2. EXPERIMENTAL

2.1. Materials

A commercial PLA grade Ingeo™ biopolymer 6201D was obtained from NatureWorks (Minnetonka, Minnesota, USA). This is a PLA grade with a density of 1.24 g cm^{-3} and a met flow rate (MFR) of 15-30 g/10 min measured at 210 ºC which makes it suitable for injection molding. AESO was supplied by Sigma Aldrich S.A. (Madrid, Spain). This commercial grade comes with 4,000 ppm hydroquinone as inhibitor to avoid polymerization. **Fig. 1** shows the chemical process to obtain AESO from epoxidized soybean oil (ESO) by treatment with AA.

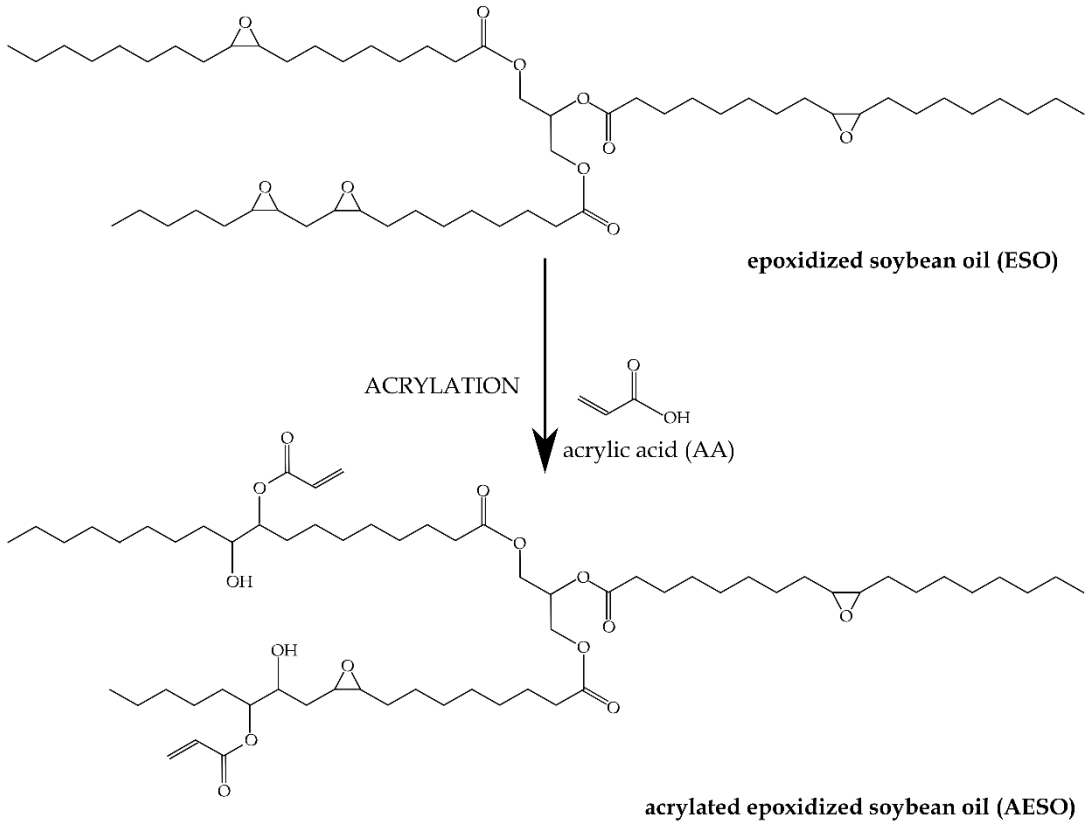

Figure 1 Schematic representation of the chemical structure of acrylated epoxidized soybean oil (AESO) obtained by acrylation of epoxidized soybean oil (ESO), previously produced from epoxidation of soybean oil (SO), with acrylic acid (AA).

2.2. Preparation of PLA parts

Prior to processing, all materials were dried in a dehumidifier MDEO from Industrial Marsé (Barcelona, Spain) at a temperature of 60 ºC for 36 h to remove residual moisture due to the high sensitiveness of PLA to hydrolysis. The AESO content varied in the 0-10 wt% range as summarized in **Table 1**.

The PLA and AESO formulations were then melt compounded in a co-rotating twin-screw extruder from Dupra, S.L. (Alicante, Spain) with a diameter of 25 mm and a length/diameter (L/D) ratio of 24. The temperature profile of the barrel was set to 180 ºC (feeding zone), 185 ºC, 190 ºC, and 195 ºC (die) and the rotating speed was 20 rpm. The extruded materials were pelletized and subsequently shaped into plastic parts by injection molding by means of a Sprinter 11t from Erinca S.L (Barcelona, Spain) using a temperature profile of 165 ºC (hopper), 170 ºC, 175 ºC, and 180 ºC (injection nozzle).

Table 1

2.3. Mechanical characterization

Mechanical properties of AESO-toughened PLA parts were obtained by both tensile and flexural tests in a universal test machine ELIB 50 from S.A.E. Ibertest (Madrid, Spain), equipped with a load cell of 5 kN. Tensile tests followed the guidelines of the ISO527-1:2012 while flexural tests were carried out as recommended by ISO 178:2011. The cross-head speed was set to 5 mm min^{-1} for both tests.

Shore hardness of the injection-molded parts was measured in a 676-D durometer from J. Bot Instruments (Barcelona, Spain), using the D-scale as recommended in ISO 868:2003. Toughness was also studied on the un-notched samples using the Charpy impact test with a 6-J pendulum from Metrotec S.A. (San Sebastián, Spain) following the

guidelines of the ISO 179-1:2010. All samples were tested at room temperature and at least six samples per formulation were evaluated to obtain the average values of the corresponding parameters.

2.4. Thermal characterization

Main thermal transitions, *i.e.* glass transition (T_g), cold crystallization (T_c), and melting (T_m) of the injection-molded parts were obtained using differential scanning calorimetry (DSC) with a Mettler-Toledo 821 calorimeter (Schwerzenbach, Switzerland). The average sample weight ranged from 5 to 7 mg and it was placed in standard aluminium crucibles with a volume capacity of 40 μL. Thermal analysis was programmed as follows: initial heating scan from 30 ºC to 200 ºC at 10 ºC min^{-1}, then a cooling scan from 200 ºC down to 0 ºC at 10 ºC min^{-1}, and finally a second heating scan from 0 ºC to 350 ºC at 10 ºC min^{-1}. All tests were run under nitrogen atmosphere with a flow-rate of 66 mL min^{-1}. In addition to above-mentioned temperatures, the degree of crystallinity (X_c) was calculated by using the following equation (**Eq. 1**):

$$X_C = \left[\frac{\Delta H_m - \Delta \boldsymbol{H_{CC}}}{\Delta H_m^0 \cdot (1-w)}\right] \cdot 100 \qquad \textbf{Equation 1}$$

Where ΔH_m and ΔH_{CC} (J g^{-1}) correspond to the enthalpies of melting and cold crystallization, respectively. ΔH_m^0 (J g^{-1}) stands for the melting enthalpy of a fully crystalline PLA, with a value of 93.0 J g^{-1} [63], and *w* represents the weight fraction of AESO in the PLA formulation.

The effect of AESO on the overall thermal stability up to decomposition was studied by thermogravimetric analysis (TGA) in a TGA/SDTA 851 thermobalance from

Mettler-Toledo, LLC (Columbus, Ohio, USA). The samples weight ranged 5-7 mg and these were placed on standard aluminum oxide (Al_2O_3) crucibles with a volume capacity of 70 μL. A dynamic heating program from 30 ºC to 700 ºC at a heating rate of 20 ºC min^{-1} in air atmosphere was used.

2.5. Thermomechanical characterization

Dynamic mechanical thermal characterization (DMTA) was performed using an AR-G2 oscillatory rheometer from TA Instruments (New Castle, Delaware, USA), equipped with a clamp system for solid samples working in torsion/shear mode. The samples, with a size of 4x10x40 mm^3, were subjected to a temperature sweep from 30 º up to 140 ºC at a constant heating rate of 2 ºC min^{-1}. The maximum deformation percentage (γ) was set to 0.1%. The storage modulus (G') and the dynamic damping factor (tan δ) were obtained as a function of temperature at a constant frequency of 1 Hz.

Thermomechanical properties were further analyzed by means of Vicat softening temperature (VST) and heat deflection temperature (HDT) tests in a Vicat/HDT station model VHDT 20 from Metrotec S.A. (San Sebastián, Spain). VST values were obtained according to ISO 306 using the B50 method, with an applied load of 50 N and a heating rate of 50 ºC h^{-1}. HDT measurements were carried out following ISO 75-1 on samples sizing 4x10x80 mm^3. The distance between supports was 60 mm and the applied force was 320 g while the heating rate was 120 ºC h^{-1}.

In addition, the dimensional stability was studied by thermomechanical analysis (TMA) in a thermomechanical analyzer Q400 from TA Instruments on samples with a size of 10x10x4 mm^3. A dynamic heating program from 0 ºC to 140 ºC at a constant heating rate of 2 ºC min^{-1} was used to obtain the coefficient of linear thermal expansion (CLTE) using a constant load of 0.02 N. All samples were tested in triplicate.

2.6. Morphology

The morphology of the injection-molded parts was observed on their fracture surfaces from impact tests. For this, field emission scanning electron microscopy (FESEM) in a ZEISS ULTRA 55 from Oxford Instruments (Abingdon, United Kingdom) was performed. The working distance (WD) varied in the 6-7 mm range and an extra high tension (EHT) of 2 kV was applied to the electron beam. Due to the non-conducting nature of the samples, these were subjected to a sputtering process with a gold-palladium alloy in a sputter coater EMITECH-SC7620 from Quorum Technologies, Ltd. (East Sussex, United Kingdom).

3. RESULTS AND DISCUSION

3.1. Mechanical properties of AESO-containing PLA parts

Fig. 2 shows the evolution of tensile properties of the injection-molded PLA parts varying the AESO content. As it can be observed in the graph, the incorporation of AESO induced a slight increase in the tensile modulus, *i.e.* from 2 GPa (for the neat PLA part) to 2.2 GPa (for PLA parts containing 10 wt% AESO). Regarding tensile strength, the neat PLA part was characterized by a value of 66 MPa. One can observe a slight decrease in tensile strength with increasing the AESO content. However, tensile strength remained relatively constant at high values, *i.e.* 63-64 MPa, for up to 7.5 wt% AESO, and a significant decrease (below 60 MPa) was only noticed at the highest content, *i.e.* 10 wt%. A similar effect was previously reported in the study carried out by Mauck *et al.* [55] in which PLA films containing 5 wt% AESO were prepared by solvent casting following by drying at 190 ºC.

Incorporation of AESO into PLA led to a considerable increase in elongation at break. The highest value of elongation at break was observed for the PLA parts containing

10 wt% AESO. In particular, this value was 10.6%, representing a percentage increase of 113% in comparison to the unmodified PLA part. Mauck *et al.* [55] previously reported a remarkable increase in elongation at break, from 4.1%, for a neat PLA film, up to 31%, for PLA films with 5 wt% AESO. This increment is substantially higher than the reported values herein for the same AESO content. However, this previous study also reported high variability on the mechanical properties, which was ascribed to the lack of homogeneity of the manufacturing process. A similar plasticizing effect was also reported by Ferri *et al.* [51] for PLA formulations containing 10-13 wt% MLO, showing an increase in elongation at break of up to 70-80%. Nevertheless, a remarkable decrease in tensile strength, in particular from 64 MPa down to 40 MPa, was also observed. Carbonell-Verdu *et al.* [52] similarly reported a ductility improvement on PLA films by means of MCSO, showing an increment in elongation at break of 11%. However, a reduction in the tensile strength of 24% was also observed. Therefore, these previous plasticizers promoted certain decrease in both the strength and modulus of PLA materials. Interestingly, the here-developed PLA parts showed a similar mechanical strength for AESO contents up to 7.5 wt% than the neat PLA part, while maintaining a similar improvement in ductility than previously studied plasticizers.

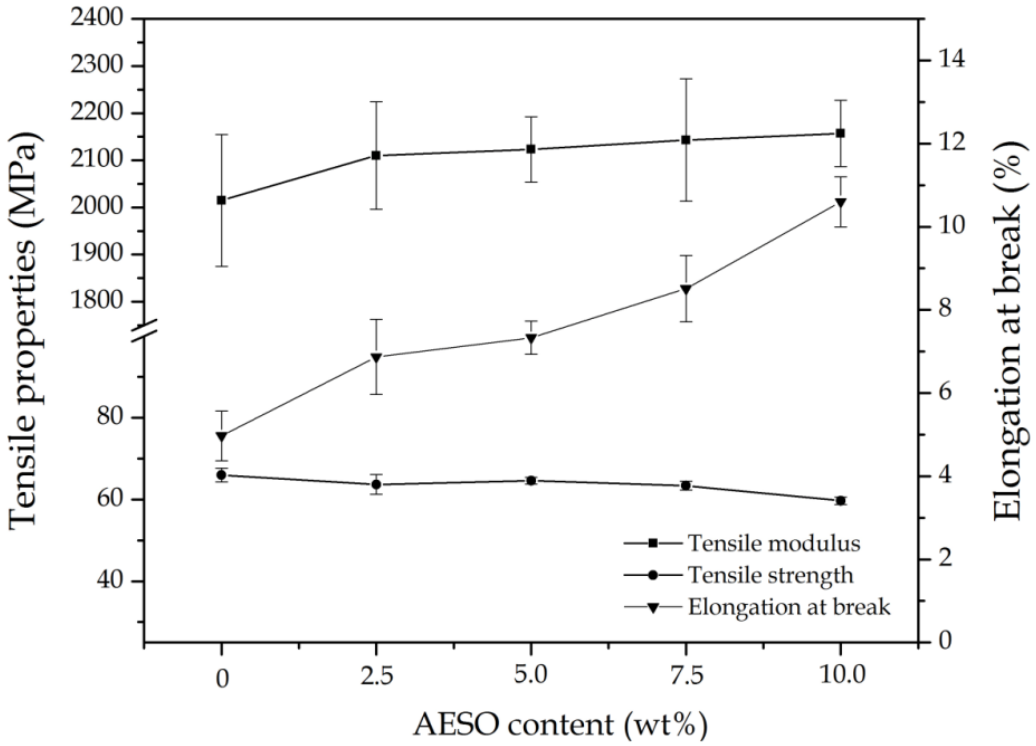

Figure 2 Plot evolution of the tensile properties of the injection-molded polylactide (PLA) parts varying the acrylated epoxidized soybean oil (AESO) content.

Fig. 3 shows the flexural properties of the PLA parts containing AESO. In relation to the flexural modulus, a slight increase from 3.3 GPa (neat PLA part) up to 3.4-3.5 GPa (for PLA parts containing 7.5-10 wt% AESO) was observed. One can also observe in the graph that AESO improved flexural strength. In particular, flexural strength increased from 89.9 MPa, for the neat PLA part, up to 100.7 MPa, for the PLA part with 10 wt% AESO. This somewhat suggests an interaction between the multiple acrylic functionalities of AESO with the PLA chains. In this sense, Mauk *et al.* [55] suggested a potential cross-linking reaction of AESO during melt processing at high temperature. Therefore, this mechanism can be responsible for the above-described mechanical

performance, *i.e.* a significant ductility improvement in combination to a moderate increase in the mechanical resistant properties.

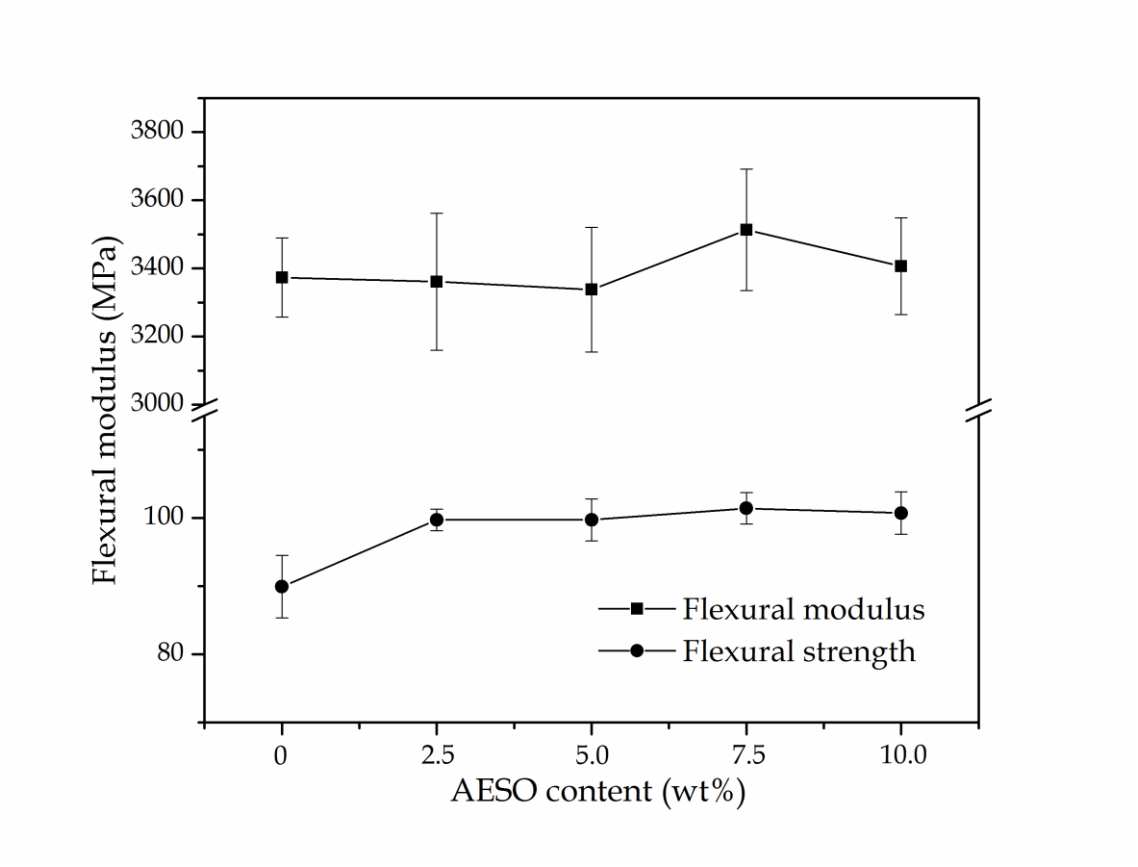

Figure 3 Plot evolution of the flexural properties of the injection-molded polylactide (PLA) parts varying the acrylated epoxidized soybean oil (AESO) content.

In relation to hardness, no significant changes were observed for the Shore D measurements of the AESO-toughened PLA parts (see **Table 2**). In general, all PLA parts showed values around 79, except the sample containing 2.5 wt%, which presented a slight increase up to approximately 81. The PLA parts containing AESO also presented a remarkable increase in toughness, as measured through the Charpy impact test. Whereas the neat PLA part showed a Charpy impact resistance of 19.5 kJ m^{-2}, the addition of only 2.5 wt% AESO increased the impact-absorbed energy up to 30.6 kJ m^{-2}, *i.e.* an increase of about 57%. The impact-strength values gradually improved up to 35.1 kJ m^{-2} for the

PLA parts containing AESO at 10 wt%. This further confirms the high effect of AESO on the toughness of the PLA parts. Similar findings were previously reported by Ferri *et al.* [51] for MLO-plasticized PLA materials, showing an increase in the absorbed energy from 30.9 kJ m^{-2}, for neat PLA, to 62.9 kJ m^{-2}, for PLA materials with 3.6 wt% MLO. This previous study also pointed out that plasticizer saturation habitually occurs at relatively low concentrations, inducing a negative effect on the overall mechanical properties. Plasticizer saturation was also observed in PLA formulations containing EFAE in the same range of concentrations, which was detectable by a clear phase separation [44]. In the present study, however, the impact-strength values of the PLA parts linearly increased with the AESO content for all studied formulations. In this sense, Nagarajan *et al.* [64] also reported interesting results in polytrimethylene terephthalate (PTT)/PLA blends by reactive compatibilization with an acrylic terpolymer, showing a remarkable increase in toughness.

Table 2

3.2. Morphology of AESO-containing PLA parts

Mechanical properties are directly related to the material-specific morphology. **Fig. 4** gathers the FESEM images, taken at 500x, of the fracture surfaces of the neat PLA and AESO-toughened PLA parts after the Charpy impact tests. As shown in **Fig. 4a**, the neat PLA part is a rigid material, showing the fracture surface morphology of a typical brittle polymer in which micro-crack formation and growth can be observed. One can also observe that there was no evidence of plastic deformation due to the intrinsic brittleness of PLA, which is related to its low energy absorption, as mentioned above. However, as it can be observed from **Fig. 4b** to **Fig. 4e**, the morphology of the fracture

surfaces of all AESO-toughened parts was remarkably different. The fracture surface changed from brittle to ductile, showing different flat levels with a certain degree of plastic deformation. Nevertheless, it is also worth to mention the presence of small spherical voids, which were more noticeable as the AESO content increased (see for instance **Fig. 4e**). The presence of these droplets suggests phase separation that is known to exert two opposing effects on a polymer matrix. On the one hand, this phenomenon occurs due to a given additive saturation that may cause migration. As a result, it has a negative influence on the mechanical properties, which has been already observed in PLA and other bio-based polyesters [44, 48, 51, 52]. On the other hand, an excess of plasticizer can also change the morphology of the material matrix. In particular, the presence of small droplets with a spherical shape can positively contribute to improve toughness as, for instance, polybutadiene rubbers (BR) do in high-impact polystyrene (HIPS). Both phenomena can occur and overlap. Their overall effect depends on the droplet size, distribution, potential interactions, etc. This phenomenon has been previously observed in PPG-plasticized PLA formulations [31].

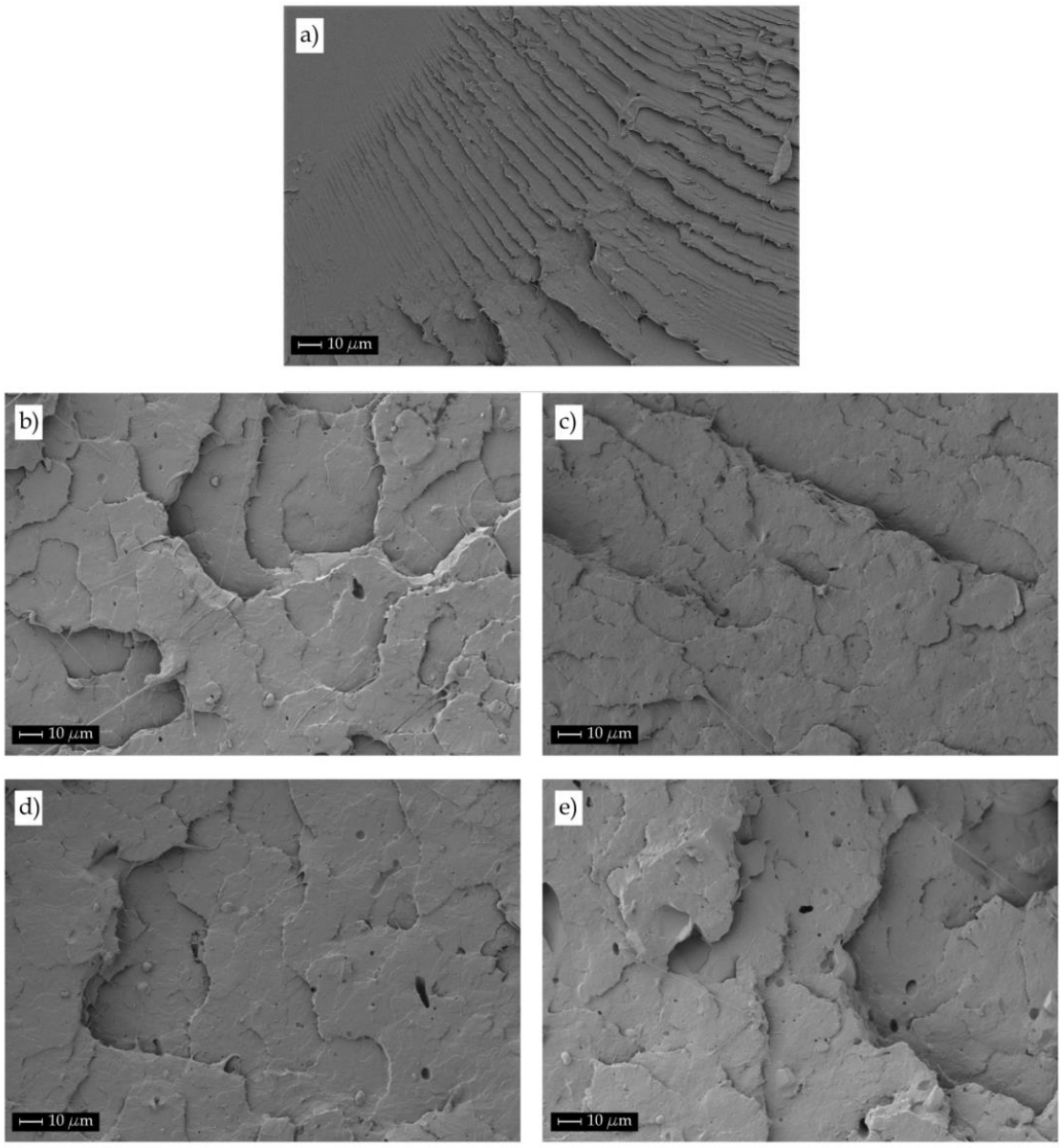

Figure 4 Field emission scanning electron microscopy (FESEM) images of the surface fractures of the injection-molded polylactide (PLA) parts with acrylated epoxidized soybean oil (AESO) taken at 500x: a) neat PLA; b) 2.5 wt% AESO; c) 5.0 wt% AESO; d) 7.5% AESO; e) 10.0 wt% AESO. Scale markers of 10 μm.

Fig. 5 shows the FESEM images taken at higher magnifications, *i.e.* 2,000x and 5,000x. These micrographs confirm, in a clear way, the morphology of the fracture surfaces of the injection-molded PLA parts. At 2,000x, some spherical holes with a mean

diameter of 1-2 μm can be observed in both parts of PLA with 2.5 wt% (**Fig. 5a**) and 10 wt% (**Fig. 5c**) AESO. The plasticizing effect exerted by AESO on the PLA matrix was supported by the presence of some filaments on the flat fracture planes resulting from plastic deformation. FESEM images taken at 5,000x confirmed phase separation at high AESO contents. PLA parts with 2.5 wt%, shown in **Fig. 5b**, presented some spherical voids but the overall surface was quite homogeneous, thus indicating good miscibility. Nevertheless, PLA parts containing 10 wt% AESO, in **Fig. 5d**, showed a noticeably phase separation since small droplets below 0.5 μm can be easily identified. Despite this, the sizes of these AESO droplets were relatively low, producing the above-described positive effect on the mechanical ductile properties. Similar findings were reported by Mauck *et al.* [55] for AESO-toughened PLA films at 5 wt%, which presented higher miscibility and then lower phase separation than soybean oil. In fact, it was reported a droplet size of 4.5 μm for the PLA films containing soybean oil while the films made of PLA with AESO at 5 wt% presented a droplet size of 2.2 μm. Ferri *et al.* [44] also observed phase separation in PLA plasticized with 13 wt% EFAE with droplet sizes similar to those observed in the here-prepared developed materials, *i.e.* around 1 μm. Therefore, this particular morphology based on submicron AESO droplets finely dispersed in the PLA matrix can be certainly responsible for the achieved toughness improvement.

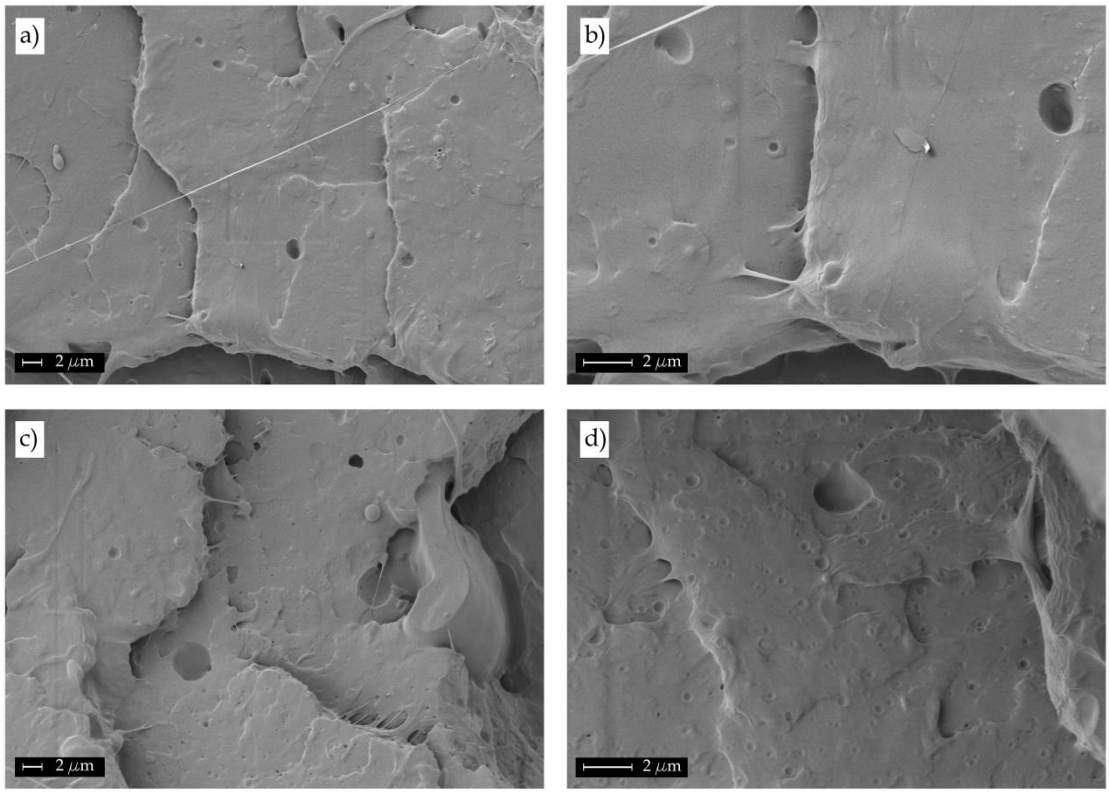

Figure 5 Field emission scanning electron microscopy (FESEM) images of the surface fractures of the injection-molded polylactide (PLA) parts with acrylated epoxidized soybean oil (AESO) taken at different magnifications: a) 2.5 wt% AESO at 2,000x; b) 2.5 wt% AESO at 5,000x; c) 10 wt% AESO at 2,000x; d) 10 wt% AESO at 5,000x. Scale markers of 2 μm.

3.3. Thermal properties of AESO-containing PLA parts

DSC thermograms for neat PLA and AESO-toughened PLA parts are shown in **Fig. 6**. A baseline step located between 60–70 ºC corresponds to T_g of PLA. The exothermic peak located between 90 ºC and 120 ºC stands for the cold crystallization process due to the rearrangement of the PLA polymer chains in a packed structure during heating. Finally, the melting process was observed in the 150–170 ºC range. As it can be seen in the thermograms, the addition of AESO shifted the cold crystallization process to

higher temperatures, which is not the usual effect of a plasticizer. That was particularly noticeable for the PLA part containing 2.5 wt% AESO. In general, a plasticizer increases free volume and reduces the polymer-polymer interactions, allowing higher chain mobility and lowering T_{CC} values [23, 46]. This unexpected anti-nucleating effect of AESO on PLA materials suggests that certain chain extension or cross-linking occurred due to its multiple acrylate and epoxy functionalities, thus leading to a chain mobility restriction. This effect was more intense for the PLA part containing 2.5 wt% AESO, as it can be seen in **Fig. 6**. At higher AESO contents, however, its plasticizing effect overlapped the chain extension/cross-linking process resulting in a decrease in cold crystallization. Therefore, the AESO-containing PLA parts at 5-10 wt% presented intermediate T_{CC} values. Similar phenomenon was previously observed by Choi *et al.* [36] by using poly(ethylene glycol) acrylate (PEGA) as additive in toughened PLA formulations. However, it is also worth to note that these previous formulations were processed with a radical initiator that promoted reactive extrusion with PLA polymer chains.

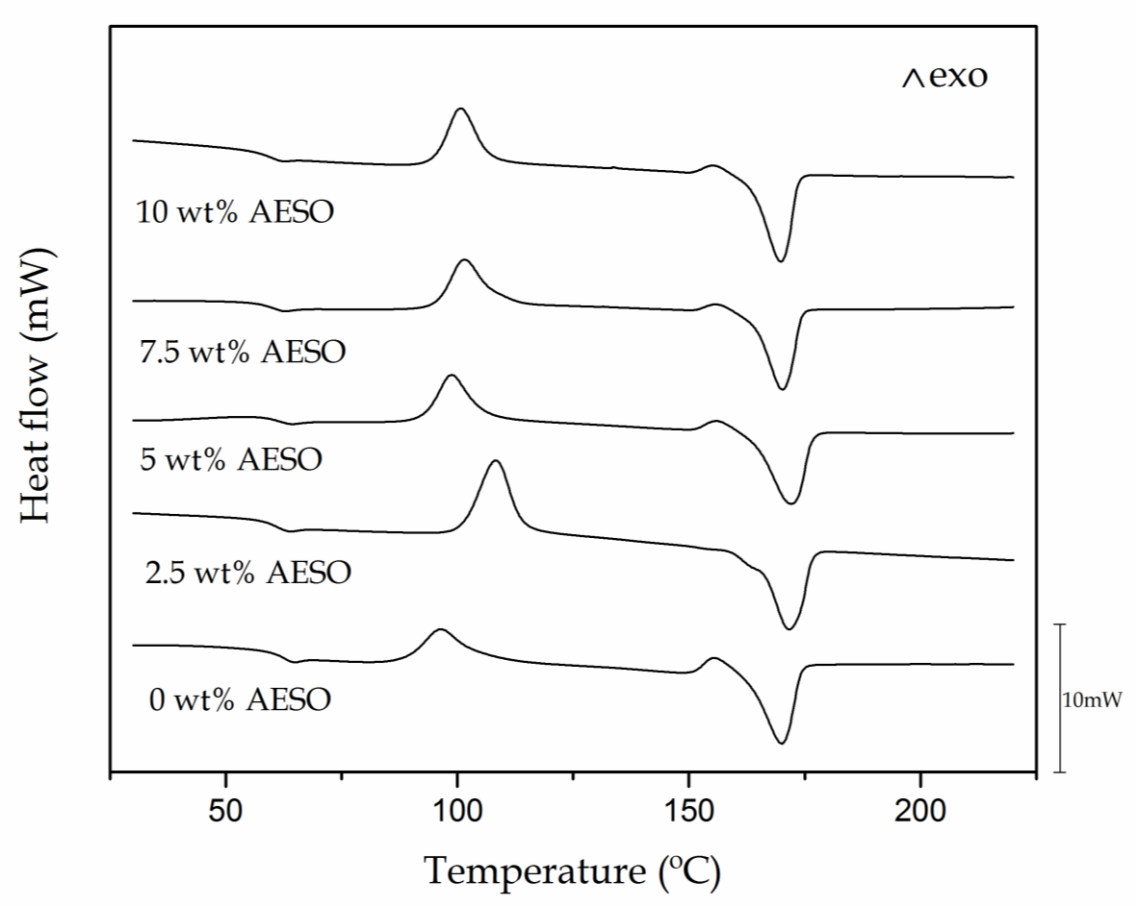

Figure 6 Comparative plot of differential scanning calorimetry (DSC) thermograms of the injection-molded polylactide (PLA) parts varying the acrylated epoxidized soybean oil (AESO) content.

The main thermal properties of the AESO-toughened PLA formulations are summarized in **Table 3**. It is worthy to note the relatively low decrease observed in the T_g values from 62.8 ºC, for the neat PLA part, to 59.4 ºC, *i.e.* a reduction of 2-3 ºC. Indeed, the efficiency of a given plasticizer is habitually directly related to their ability to lower polymer T_g. The obtained results further confirm that AESO does not play the typical plasticization role in PLA. In fact, other plasticizers, such as PEG, ATBC, PPG, OLAs, etc., are known to be capable to decrease T_g by 25–30 ºC with a plasticizer content in the 10–20 wt% range [23, 26, 31, 33]. Similar findings were reported by Mauck *et al.* [55] in plasticized PLA by 5 wt% AESO, showing a T_g decrease of *ca.* 1 ºC with regard to the

unplasticized PLA film. This can be related to the restricted chain motion to form a packed structure with AESO addition. Regarding the cold crystallization process, as above described, this occurred at higher temperatures. In particular, T_{CC} increased from 96.3 ºC, for the neat PLA part, to up 105.9 ºC, for the PLA part containing 2.5 wt% AESO. Another important observation was the X_C decrease. This reduction was particularly high for the PLA part formulated with 2.5 wt%, supporting the chain extension/cross-linking process between the acrylate and epoxy groups and the hydroxyl groups of the PLA chains. However, even though the degree of crystallization was reduced, the mechanical strength of the PLA parts toughened by AESO was similar to that of the neat PLA part.

Table 3

Another important feature that AESO provided to the PLA parts was an improvement on thermal stability, which can be observed in **Fig. 7**. This is an interesting result since one of the main drawbacks of most plasticizers (*e.g.* PEG, PPG, ATBC, etc.) is that they contribute to lower the thermal stability of PLA [23, 36]. Thermal stability impairment is habitually related to a process of plasticizer evaporation, which becomes especially important for additives of low M_W that are not clearly detected by DSC. However, this phenomenon can be easily detected by TGA, allowing to evaluate whether the additive improves or not the thermal stability. This is a key issue in defining the processing window of PLA formulations, which are typically processed at 180–190 ºC or even at higher temperatures, being thus necessary to ensure that plasticizer evaporation does not occur in this temperature range. Moreover, TGA also gave evidence of the thermal stabilization effect that AESO provides to PLA. As reported by Carrasco *et al.* [65, 66], PLA degradation habitually occurs in a single step, following a chain scission

mechanism. It was also reported an increase in thermal stability by using reactive extrusion, which gave partially branched PLA chains [67]. **Fig. 7a** shows a comparison plot of the TGA thermograms of the neat PLA and AESO-toughened PLA parts varying the AESO content. Inset in **Fig. 7a** shows a detailed graph of the degradation onset. It is clearly observable the displacement of the degradation curves to higher temperatures. The decomposition process proceeded in a one-stage weight loss for all PLA materials as it can be concluded from the derivative thermogravimetric (DTG) curves (see **Fig. 7b**). The most striking fact is that AESO increased thermal stability at high temperatures, thus leading to a significant delay in the degradation process. Degradation temperature (T_{deg}), corresponding to the maximum degradation rate and shown by the temperature peak in the DTG graphs, increased from is 361 ºC, for the neat PLA part, up to 370 ºC, for PLA parts with 5.0–7.5 wt% AESO contents. Similar to that mentioned above during DSC characterization, the PLA part with 2.5 wt% AESO showed a slightly different thermal behavior. This AESO content also led to the highest thermal stability of all studied compositions. This is related to the fact that both overlapping effects, *i.e.* plasticization and chain extension/cross-linking, took place simultaneously and the predominance of one over the other depends on the additive amount. This feature has been also observed for other modified vegetable oils in PLA formulations and represents a positive issue with regard to other conventional plasticizing/toughening agents for bio-based polyesters [44, 46, 48, 51].

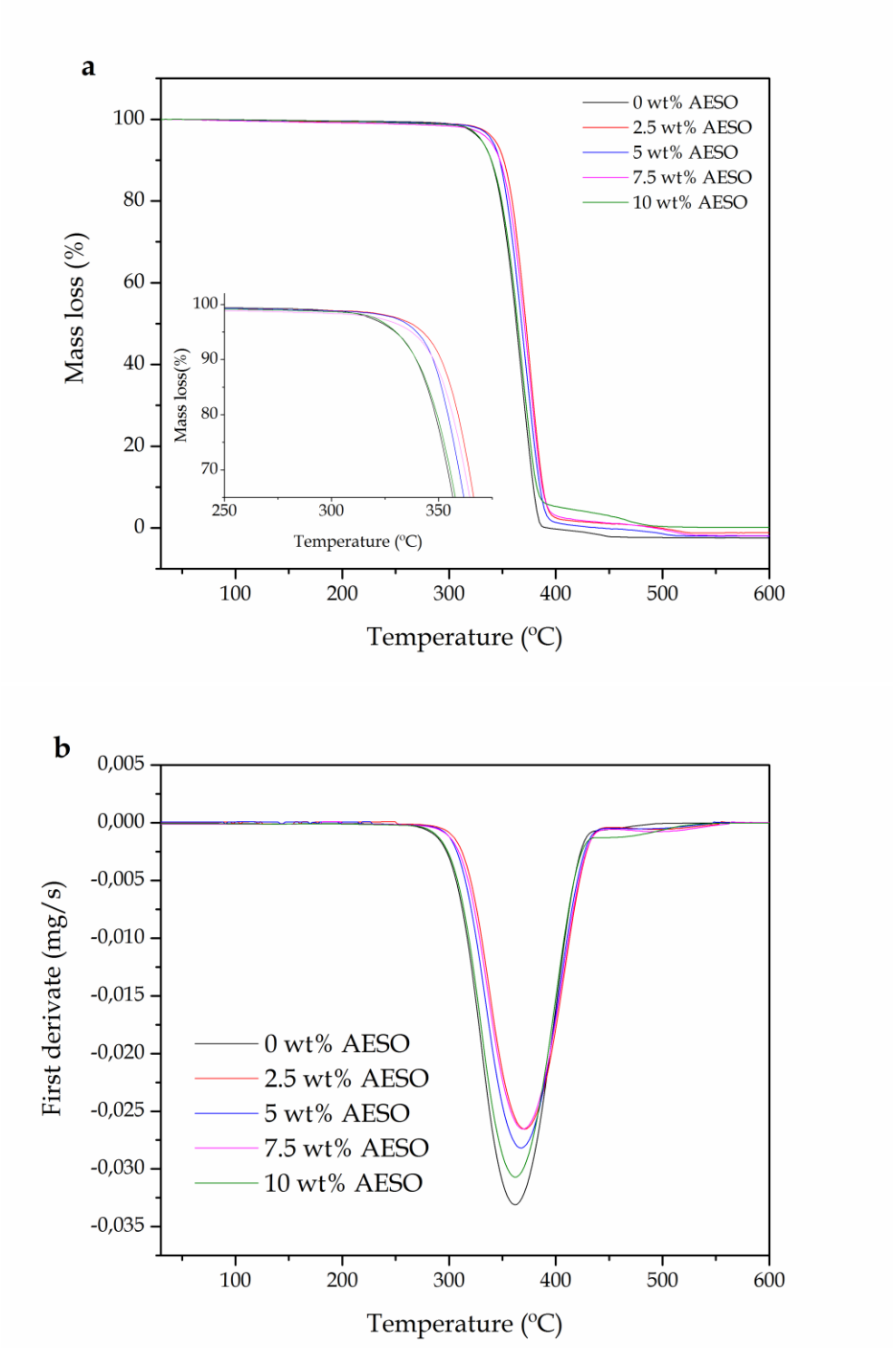

Figure 7 Thermal stability of the injection-molded polylactide (PLA) parts varying the acrylated epoxidized soybean oil (AESO) content in terms of: a) Thermogravimetric analysis (TGA) curves; b) Derivative thermogravimetric (DTG) curves.

3.4. Thermomechanical properties of AESO-containing PLA parts

With regard to DMTA analysis, **Fig. 8** gathers a comparative plot of the evolution of G' and tan δ shown in **Fig. 8a** and **8b**, respectively. In **Fig. 8a**, a two-fold reduction in G' can be observed. The curves showed a first G' decrease from 50 ºC to 70 ºC, related to T_g of PLA, followed by the cold crystallization process of the biopolymer that was discernable by a G' increase in the 75–90 ºC range. It is worthy to note that the PLA parts containing AESO presented lower G' values, which represents a positive effect on toughness. This effect was more noticeable for the PLA part with 10 wt% AESO. Furthermore, in relation to the cold crystallization process, it can be clearly observed a displacement to higher temperatures, thus indicating that AESO addition delayed the crystallization process, as previously described in the DSC analysis. **Fig. 8b** shows the evolution of tan δ, the so-called damping factor, for the neat PLA and AESO-toughened PLA parts. The α-relaxation peak, which is ascribed to the biopolymer T_g, was located in the 60–70 ºC range. One can observe that the decrease in T_g was relatively small, of about 5 ºC, as also described during DSC. Nevertheless, all AESO-containing PLA parts were characterized by higher tan δ values, which can be related to the formation of a macromolecular structure with a higher energy dissipation capacity and correlates well with the improved toughness described during mechanical analysis.

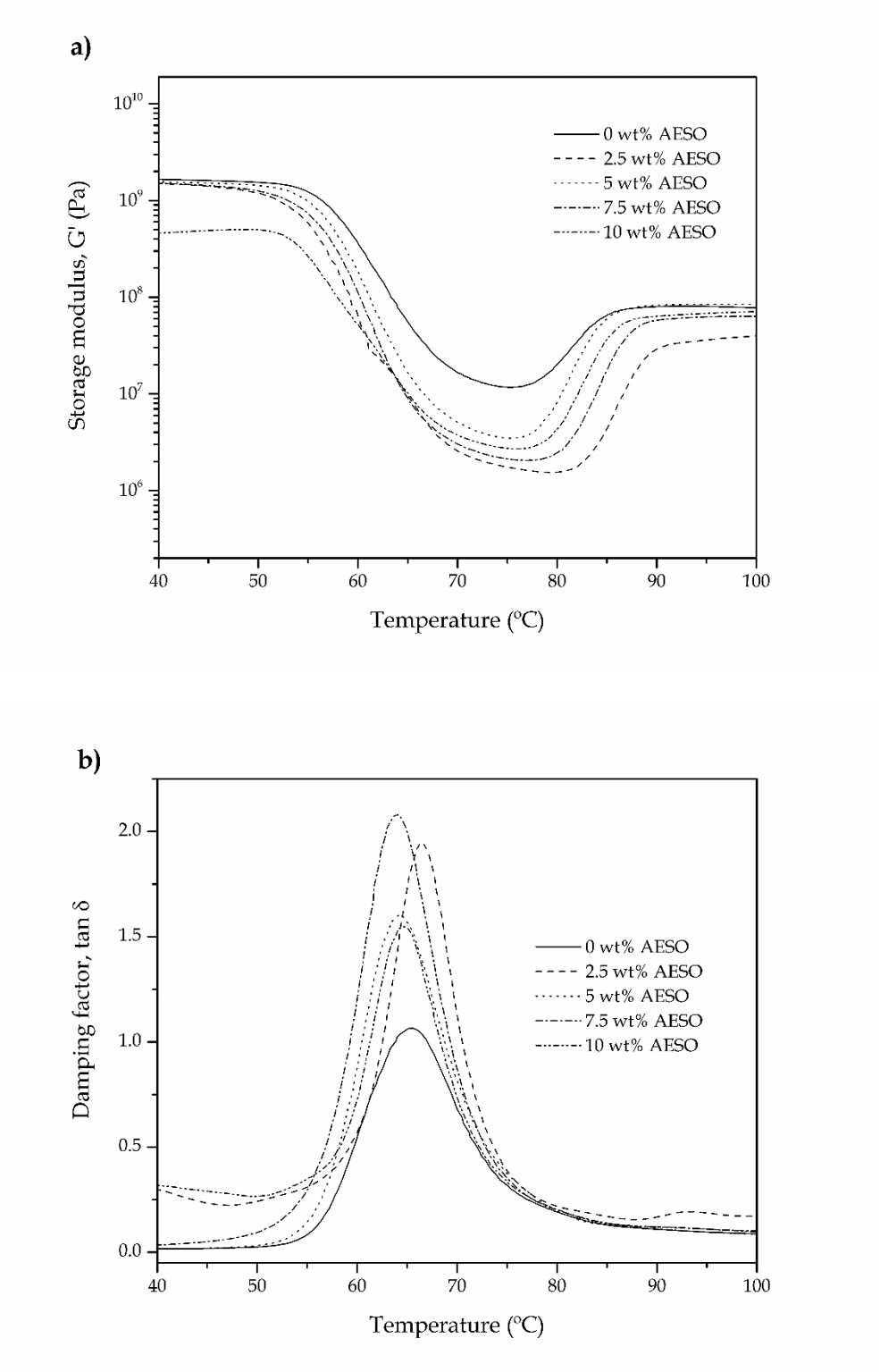

Figure 8 Dynamic mechanical thermal analysis (DMTA) curves of the injection-molded polylactide (PLA) parts varying the acrylated epoxidized soybean oil (AESO) content: a) Storage modulus (G'); b) Damping factor (tan δ).

Finally, **Table 4** shows the evolution of the CLTE values, below and above T_g, obtained by TMA. It can be observed that all PLA parts presented higher CLTE values above T_g since the movement of the biopolymer chains was favored. Below T_g, the CLTE value of the neat PLA part was 94.4 µm m^{-1} $ºC^{-1}$ and the AESO-containing PLA parts showed slightly reduced CLTE values. On the contrary, above T_g, the neat PLA part presented a CLTE value of 146.9 µm m^{-1} $ºC^{-1}$, which considerably increased for the PLA parts with AESO. This phenomenon correlates well with the previously described mechanical and thermomechanical properties. Dimensional stability was measured by means of other two thermomechanical parameters, *i.e.* VST and HDT, which are also included in **Table 4**. One can observe that VST and HDT values for the neat PLA part were 56.3 ºC and 55.4 ºC, respectively, and these thermomechanical values were slightly lower after AESO addition. In fact, the decrease observed in VST and HDT was in the 2–3 ºC range, thus indicating an extraordinary thermomechanical response.

Table 4

4. CONCLUSIONS

In the present study, AESO has been proposed as a novel additive for toughening PLA parts obtained by injection molding. Although the plasticizing effect of AESO in terms of T_g decrease was not remarkable, PLA toughness was noticeably improved. In particular, AESO had a positive effect on elongation at break, which increased from 4.97 %, for the neat PLA part, up to 10.6%, for the PLA part with 10 wt% AESO, though the most balanced performance was observed for an AESO content of 2.5 wt%. Furthermore, the mechanical strength of the AESO-toughened PLA parts was in the same range of the neat PLA part more likely due to a chain-extension and/or cross-linking process of the

biopolymer chains induced by the acrylate and epoxy groups present in AESO. Additionally, impact strength increased from 19.5 kJ m^{-2}, for the neat PLA part, up to 35.1 kJ m^{-2}, for the PLA part with 10 wt% AESO. FESEM analysis also revealed good miscibility, in particular for the lowest AESO concentration (2.5 wt%) while AESO saturation occurred at concentrations above 7.5 wt%. The fracture surfaces showed a characteristic morphology defined by a PLA-rich matrix phase in which submicron spherical droplets of AESO appeared fully dispersed. With regard to the thermal properties, AESO addition favored the formation of a more amorphous structure and increased thermal stability of PLA as evidenced by DSC and TGA analysis, respectively. In addition, the thermomechanical measurements indicated that the AESO-containing PLA parts can be applied in technical applications at similar temperatures than the neat PLA part. Therefore, AESO represents an environmentally friendly solution to reduce the intrinsic brittleness of PLA materials, widening and balancing their performance. These toughened PLA parts can be particularly interesting for rigid packaging, automotive or building and construction applications, in which elastic materials but with enhanced ductility and sufficient impact strength are highly demanded.

ACKNOWLEDGEMENTS

Funding: This work was supported by the Spanish Ministry of Economy and Competitiveness (MINECO) [grant numbers MAT2014-59242-C2-1-R & AGL2015-63855-C2-1-R]. L. Quiles-Carrillo thanks the Spanish Ministry of Education, Culture, and Sports (MECD) for financial support through the FPU program [grant number FPU15/03812].

REFERENCES

[1] M.P. Arrieta, M.D. Samper, M. Aldas, J. Lopez, On the Use of PLA-PHB Blends for Sustainable Food Packaging Applications, Materials 10 (2017) 26.

[2] P.K. Bajpai, I. Singh, J. Madaan, Development and characterization of PLA-based green composites: A review, J. Thermoplast. Compos. 27 (2014) 52-81.

[3] J.S. Bergstrom, D. Hayman, An Overview of Mechanical Properties and Material Modeling of Polylactide (PLA) for Medical Applications, Ann. Biomed. Eng. 44 (2016) 330-340.

[4] J. Jozwicka, K. Gzyra-Jagiela, A. Gutowska, K. Twarowska-Schmidt, M. Cieplinski, Chemical Purity of PLA Fibres for Medical Devices, Fibres Text. East Eur. 20 (2012) 135-141.

[5] D. Notta-Cuvier, J. Odent, R. Delille, M. Murariu, F. Lauro, J.M. Raquez, B. Bennani, P. Dubois, Tailoring polylactide (PLA) properties for automotive applications: Effect of addition of designed additives on main mechanical properties, Polym. Test. 36 (2014) 1-9.

[6] N. Herrera, H. Roch, A.M. Salaberria, M.A. Pino-Orellana, J. Labidi, S.C.M. Fernandes, D. Radic, A. Leiva, K. Oksman, Functionalized blown films of plasticized polylactic acid/chitin nanocomposite: Preparation and characterization, Mater. Des. 92 (2016) 846-852.

[7] G.E. Luckachan, C.K.S. Pillai, Biodegradable Polymers- A Review on Recent Trends and Emerging Perspectives, J. Polym. Environ. 19 (2011) 637-676.

[8] J.M. Chacon, M.A. Caminero, E. Garcia-Plaza, P.J. Nunez, Additive manufacturing of PLA structures using fused deposition modelling: Effect of process parameters on mechanical properties and their optimal selection, Mater. Des. 124 (2017) 143-157.

[9] A. Le Duigou, M. Castro, R. Bevan, N. Martin, 3D printing of wood fibre biocomposites: From mechanical to actuation functionality, Mater. Des. 96 (2016) 106-114.

[10] A. Tsouknidas, M. Pantazopoulos, I. Katsoulis, D. Fasnakis, S. Maropoulos, N. Michailidis, Impact absorption capacity of 3D-printed components fabricated by fused deposition modelling, Mater. Des. 102 (2016) 41-44.

[11] H. Balakrishnan, A. Hassan, M.U. Wahit, A.A. Yussuf, S.B.A. Razak, Novel toughened polylactic acid nanocomposite: Mechanical, thermal and morphological properties, Mater. Des. 31 (2010) 3289-3298.

[12] H.Z. Liu, J.W. Zhang, Research Progress in Toughening Modification of Poly(lactic acid), J. Polym. Sci. Pol. Phys. 49 (2011) 1051-1083.

[13] M. Wang, Y. Wu, Y.D. Li, J.B. Zeng, Progress in Toughening Poly(Lactic Acid) with Renewable Polymers, Polym. Rev. 57 (2017) 557-593.

[14] M.R. Aghjeh, M. Nazari, H.A. Khonakdar, S.H. Jafari, U. Wagenknecht, G. Heinrich, In depth analysis of micro-mechanism of mechanical property alternations in PLA/EVA/clay nanocomposites: A combined theoretical and experimental approach, Mater. Des. 88 (2015) 1277-1289.

[15] W.R. Jiang, R.Y. Bao, W. Yang, Z.Y. Liu, B.H. Xie, M.B. Yang, Morphology, interfacial and mechanical properties of polylactide/poly(ethylene terephthalate glycol) blends compatibilized by polylactide-g-maleic anhydride, Mater. Des. 59 (2014) 524-531.

[16] K.M. Nampoothiri, N.R. Nair, R.P. John, An overview of the recent developments in polylactide (PLA) research, Bioresource Technol. 101 (2010) 8493-8501.

[17] A.J.R. Lasprilla, G.A.R. Martinez, B.H. Lunelli, A.L. Jardini, R. Maciel, Poly-lactic acid synthesis for application in biomedical devices - A review, Biotechnol. Adv. 30 (2012) 321-328.

[18] G. Kfoury, J.M. Raquez, F. Hassouna, J. Odent, V. Toniazzo, D. Ruch, P. Dubois, Recent advances in high performance poly(lactide): from "green" plasticization to super -tough materials via (reactive) compounding, Front. Chem. 1 (2013) 46.

[19] J.B. Zeng, K.A. Li, A.K. Du, Compatibilization strategies in poly(lactic acid)-based blends, RSC Adv. 5 (2015) 32546-32565.

[20] V.P. Martino, R.A. Ruseckaite, A. Jimenez, Thermal and mechanical characterization of plasticized poly (L-lactide-co-D,L-lactide) films for food packaging, J. Therm. Anal. Calorim. 86 (2006) 707-712.

[21] M. Baiardo, G. Frisoni, M. Scandola, M. Rimelen, D. Lips, K. Ruffieux, E. Wintermantel, Thermal and mechanical properties of plasticized poly(L-lactic acid), J. App. Polym. Sci. 90 (2003) 1731-1738.

[22] M.P. Arrieta, E. Fortunati, F. Dominici, J. Lopez, J.M. Kenny, Bionanocomposite films based on plasticized PLA-PHB/cellulose nanocrystal blends, Carbohyd. Polym. 121 (2015) 265-275.

[23] M.P. Arrieta, M.D. Castro-Lopez, E. Rayon, L.F. Barral-Losada, J.M. Lopez-Vilarino, J. Lopez, M.V. Gonzalez-Rodriguez, Plasticized Poly(lactic acid)-Poly(hydroxybutyrate) (PLA-PHB) Blends Incorporated with Catechin Intended for Active Food-Packaging Applications, J. Agr. Food Chem. 62 (2014) 10170-10180.

[24] M. Maiza, M.T. Benaniba, G. Quintard, V. Massardier-Nageotte, Biobased additive plasticizing Polylactic acid (PLA), Polimeros 25 (2015) 581-590.

[25] S.B. Park, S.Y. Hwang, C.W. Moon, S.S. Im, E.S. Yoo, Plasticizer Effect of Novel PBS Ionomer in PLA/PBS Ionomer Blends, Macromol. Res. 18 (2010) 463-471.

[26] N. Burgos, V.P. Martino, A. Jimenez, Characterization and ageing study of poly(lactic acid) films plasticized with oligomeric lactic acid, Polym. Degrad. Stabil. 98 (2013) 651-658.

[27] I. Armentano, E. Fortunati, N. Burgos, F. Dominici, F. Luzi, S. Fiori, A. Jimenez, K. Yoon, J. Ahn, S. Kang, J.M. Kenny, Processing and characterization of plasticized PLA/PHB blends for biodegradable multiphase systems, Express Polym. Lett. 9 (2015) 583-596.

[28] M.P. Arrieta, J. Lopez, E. Rayon, A. Jimenez, Disintegrability under composting conditions of plasticized PLA-PHB blends, Polym. Degrad. Stabil. 108 (2014) 307-318.

[29] H.H. Ge, F. Yang, Y.P. Hao, G.F. Wu, H.L. Zhang, L.S. Dong, Thermal, Mechanical, and Rheological Properties of Plasticized Poly(L-lactic acid), J. App. Polym. Sci. 127 (2013) 2832-2839.

[30] K. Sungsanit, N. Kao, S.N. Bhattacharya, Properties of linear poly(lactic acid)/polyethylene glycol blends, Polym. Eng. Sci. 52 (2012) 108-116.

[31] Z. Kulinski, E. Piorkowska, K. Gadzinowska, M. Stasiak, Plasticization of poly(L-lactide) with poly(propylene glycol), Biomacromolecules 7 (2006) 2128-2135.

[32] E. Piorkowska, Z. Kulinski, A. Galeski, R. Masirek, Plasticization of semicrystalline poly(L-lactide) with poly(propylene glycol), Polymer 47 (2006) 7178-7188.

[33] M. Kowalczyk, M. Pluta, E. Piorkowska, N. Krasnikova, Plasticization of polylactide with block copolymers of ethylene glycol and propylene glycol, J. App. Polym. Sci. 125 (2012) 4292-4301.

[34] Y. Yang, J.C. Huang, R.Y. Zhang, J. Zhu, Designing bio-based plasticizers: Effect of alkyl chain length on plasticization properties of isosorbide diesters in PVC blends, Mater. Des. 126 (2017) 29-36.

[35] Y. Yang, Z. Xiong, L.S. Zhang, Z.B. Tang, R.Y. Zhang, J. Zhu, Isosorbide dioctoate as a "green" plasticizer for poly(lactic acid), Mater. Des. 91 (2016) 262-268.

[36] K.M. Choi, S.W. Lim, M.C. Choi, Y.M. Kim, D.H. Han, C.S. Ha, Thermal and mechanical properties of poly(lactic acid) modified by poly(ethylene glycol) acrylate through reactive blending, Polym. Bull. 71 (2014) 3305-3321.

[37] S. Torres-Giner, N. Montanes, T. Boronat, L. Quiles-Carrillo, R. Balart, Melt grafting of sepiolite nanoclay onto poly(3-hydroxybutyrate-co-4-hydroxybutyrate) by reactive extrusion with multi-functional epoxy-based styrene-acrylic oligomer, Eur. Polym. J. 84 (2016) 693-707.

[38] M.R. Islam, M.D.H. Beg, S.S. Jamari, Development of Vegetable-Oil-Based Polymers, J. App. Polym. Sci. 131 (2014) 13.

[39] A. Gandini, T.M. Lacerda, A.J.F. Carvalho, E. Trovatti, Progress of Polymers from Renewable Resources: Furans, Vegetable Oils, and Polysaccharides, Chem. Rev. 116 (2016) 1637-1669.

[40] R. Kozlowski, K. Bujnowicz, Polymers from vegetable oils, Przem. Chem. 87 (2008) 1168-1170.

[41] J.W. King, Determination of the solubility parameter os soybean oil by inverse gas-chromatography, Food Sci. Technol.-Leb 28 (1995) 190-195.

[42] M.P. Arrieta, M.D. Samper, J. Lopez, A. Jimenez, Combined Effect of Poly(hydroxybutyrate) and Plasticizers on Polylactic acid Properties for Film Intended for Food Packaging, J. Polym. Environ. 22 (2014) 460-470.

[43] Q. Wang, Y.L. Chen, J. Tang, Z.F. Zhang, Determination of the Solubility Parameter of Epoxidized Soybean Oil by Inverse Gas Chromatography, J. Macromol. Sci. Phys. 52 (2013) 1405-1413.

[44] J.M. Ferri, M.D. Samper, D. Garcia-Sanoguera, M.J. Reig, O. Fenollar, R. Balart, Plasticizing effect of biobased epoxidized fatty acid esters on mechanical and thermal properties of poly(lactic acid), J. Mater. Sci. 51 (2016) 5356-5366.

[45] M. Li, S.H. Li, J.L. Xia, C.X. Ding, M. Wang, L.N. Xu, X.H. Yang, K. Huang, Tung oil based plasticizer and auxiliary stabilizer for poly(vinyl chloride), Mater. Des. 122 (2017) 366-375.

[46] B.W. Chieng, N.A. Ibrahim, Y.Y. Then, Y.Y. Loo, Epoxidized Vegetable Oils Plasticized Poly(lactic acid) Biocomposites: Mechanical, Thermal and Morphology Properties, Molecules 19 (2014) 16024-16038.

[47] Y.Q. Xu, J.P. Qu, Mechanical and Rheological Properties of Epoxidized Soybean Oil Plasticized Poly(lactic acid), J. App. Polym. Sci. 112 (2009) 3185-3191.

[48] D. Garcia-Garcia, J.M. Ferri, N. Montanes, J. Lopez-Martinez, R. Balart, Plasticization effects of epoxidized vegetable oils on mechanical properties of poly(3-hydroxybutyrate), Polym. Int. 65 (2016) 1157-1164.

[49] J.F. Balart, V. Fombuena, O. Fenollar, T. Boronat, L. Sanchez-Nacher, Processing and characterization of high environmental efficiency composites based on PLA and hazelnut shell flour (HSF) with biobased plasticizers derived from epoxidized linseed oil (ELO), Compos. Part B-Eng. 86 (2016) 168-177.

[50] S. Torres-Giner, N. Montanes, O. Fenollar, D. García-Sanoguera, R. Balart, Development and optimization of renewable vinyl plastisol/wood flour composites exposed to ultraviolet radiation, Mater. Des. 108 (2016) 648-658.

[51] J.M. Ferri, D. Garcia-Garcia, N. Montanes, O. Fenollar, R. Balart, The effect of maleinized linseed oil as biobased plasticizer in poly(lactic acid)-based formulations, Polym. Int. 66 (2017) 882-891.

[52] A. Carbonell-Verdu, D. Garcia-Garcia, F. Dominici, L. Torre, L. Sanchez-Nacher, R. Balart, PLA films with improved flexibility properties by using maleinized cottonseed oil, Eur. Polym. J. 91 (2017) 248-259.

[53] Z. Xiong, C. Li, S.Q. Ma, J.X. Feng, Y. Yang, R.Y. Zhang, J. Zhu, The properties of poly(lactic acid)/starch blends with a functionalized plant oil: Tung oil anhydride, Carbohyd. Polym. 95 (2013) 77-84.

[54] L. Quiles-Carrillo, N. Montanes, S. Sammon, R. Balart, S. Torres-Giner, Compatibilization of highly sustainable polylactide/almond shell flour composites by reactive extrusion with maleinized linseed oil, Ind. Crops Prod. (2017) http://dx.doi.org/10.1016/j.indcrop.2017.10.062.

[55] S.C. Mauck, S. Wang, W.Y. Ding, B.J. Rohde, C.K. Fortune, G.Z. Yang, S.K. Ahn, M.L. Robertson, Biorenewable Tough Blends of Polylactide and Acrylated Epoxidized Soybean Oil Compatibilized by a Polylactide Star Polymer, Macromolecules 49 (2016) 1605-1615.

[56] N. Najafi, M.C. Heuzey, P.J. Carreau, D. Therriault, C.B. Park, Mechanical and morphological properties of injection molded linear and branched-polylactide (PLA) nanocomposite foams, Eur. Polym. J. 73 (2015) 455-465.

[57] L.T. Lim, R. Auras, M. Rubino, Processing technologies for poly(lactic acid), Prog. Polym. Sci. 33 (2008) 820-852.

[58] T. Takayama, K. Uchiumi, H. Ito, T. Kawai, M. Todo, Particle size distribution effects on physical properties of injection molded HA/PLA composites, Adv. Compos. Mater. 22 (2013) 327-337.

[59] A.M. Harris, E.C. Lee, Improving mechanical performance of injection molded PLA by controlling crystallinity, J. App. Polym. Sci. 107 (2008) 2246-2255.

[60] J.P. Mofokeng, A.S. Luyt, T. Tabi, J. Kovacs, Comparison of injection moulded, natural fibre-reinforced composites with PP and PLA as matrices, J. Thermoplast. Compos. 25 (2012) 927-948.

[61] S. Chaitanya, I. Singh, Processing of PLA/sisal fiber biocomposites using direct- and extrusion-injection molding, Mater. Manuf. Process. 32 (2017) 468-474.

[62] S. Pivsa-Art, J. Kord-Sa-Ard, W. Pivsa-Art, R. Wongpajan, N. O-Charoen, S. Pavasupree, H. Hamada, 2016, Coe on Sustainable Energy System, 89, 353-360.

[63] T. Tábi, A.Z. Égerházi, P. Tamás, T. Czigány, J.G. Kovács, Investigation of injection moulded poly (lactic acid) reinforced with long basalt fibres, Compos. Part A-Appl. S. 64 (2014) 99-106.

[64] V. Nagarajan, A.K. Mohanty, M. Misra, Reactive compatibilization of poly trimethylene terephthalate (PTT) and polylactic acid (PLA) using terpolymer: Factorial design optimization of mechanical properties, Mater. Des. 110 (2016) 581-591.

[65] F. Carrasco, L.A. Perez-Maqueda, O.O. Santana, M.L. Maspoch, Enhanced general analytical equation for the kinetics of the thermal degradation of poly(lactic acid)/montmorillonite nanocomposites driven by random scission, Polym. Degrad. Stabil. 101 (2014) 52-59.

[66] F. Carrasco, L.A. Perez-Maqueda, P.E. Sanchez-Jimenez, A. Perejon, O.O. Santana, M.L. Maspoch, Enhanced general analytical equation for the kinetics of the thermal degradation of poly(lactic acid) driven by random scission, Polym. Test. 32 (2013) 937-945.

[67] F. Carrasco, J. Cailloux, P.E. Sanchez-Jimenez, M.L. Maspoch, Improvement of the thermal stability of branched poly(lactic acid) obtained by reactive extrusion, Polym. Degrad. Stabil. 104 (2014) 40-49.

FIGURE CAPTIONS

Figure 1 Schematic representation of the chemical structure of acrylated epoxidized soybean oil (AESO) obtained by acrylation of epoxidized soybean oil (ESO), previously produced from epoxidation of soybean oil (SO), with acrylic acid (AA).

Figure 2 Plot evolution of the tensile properties of the injection-molded polylactide (PLA) parts varying the acrylated epoxidized soybean oil (AESO) content.

Figure 3 Plot evolution of the flexural properties of the injection-molded polylactide (PLA) parts varying the acrylated epoxidized soybean oil (AESO) content.

Figure 4 Field emission scanning electron microscopy (FESEM) images of the surface fractures of the injection-molded polylactide (PLA) parts with acrylated epoxidized soybean oil (AESO) taken at 500x: a) neat PLA; b) 2.5 wt% AESO; c) 5.0 wt% AESO; d) 7.5% AESO; e) 10.0 wt% AESO. Scale markers of 10 μm.

Figure 5 Field emission scanning electron microscopy (FESEM) images of the surface fractures of the injection-molded polylactide (PLA) parts with acrylated epoxidized soybean oil (AESO) taken at different magnifications: a) 2.5 wt% AESO at 2,000x; b) 2.5 wt% AESO at 5,000x; c) 10 wt% AESO at 2,000x; d) 10 wt% AESO at 5,000x. Scale markers of 2 μm.

Figure 6 Comparative plot of differential scanning calorimetry (DSC) thermograms of the injection-molded polylactide (PLA) parts varying the acrylated epoxidized soybean oil (AESO) content.

Figure 7 Thermal stability of the injection-molded polylactide (PLA) parts varying the acrylated epoxidized soybean oil (AESO) content in terms of: a) Thermogravimetric analysis (TGA) curves; b) Derivative thermogravimetric (DTG) curves.

Figure 8 Dynamic mechanical thermal analysis (DMTA) curves of the injection-molded polylactide (PLA) parts varying the acrylated epoxidized soybean oil (AESO) content: a) Storage modulus (G'); b) Damping factor (tan δ).

TABLES

Table 1.- Composition and coding of the different prepared formulations based on polylactide (PLA) and acrylated epoxidized soybean oil (AESO).

Sample	**PLA content (wt%)**	**AESO content (wt%)**
0 wt% AESO	100	0
2.5 wt% AESO	97.5	2.5
5 wt% AESO	95.0	5.0
7.5 wt% AESO	92.5	7.5
10 wt% AESO	90.0	10.0

Table 2.- Shore D hardness and Charpy impact values of the injection-molded polylactide (PLA) parts varying the acrylated epoxidized soybean oil (AESO) content.

AESO content (wt%)	**Shore D hardness**	**Charpy impact (kJ m^{-2})**
0	79.0 ± 0.6	19.5 ± 2.6
2.5	81.7 ± 0.8	30.6 ± 0.1
5.0	79.6 ± 0.9	31.9 ± 0.1
7.5	79.0 ± 0.4	33.7 ± 1.7
10.0	79.0 ± 0.5	35.1 ± 2.3

Table 3.- Thermal properties obtained from the differential scanning calorimetry (DSC) curves in terms of glass transition temperature (T_g), cold crystallization temperature (T_{CC}), enthalpy of crystallization (ΔH_{CC}), melting temperature (T_m), enthalpy of melting (ΔH_m), and degree of crystallinity (X_c) for the injection-molded polylactide (PLA) parts varying the acrylated epoxidized soybean oil (AESO) content.

AESO content (wt%)	**T_g (ºC)**	**T_{CC} (ºC)**	**ΔH_{CC} (J g^{-1})**	**T_m (ºC)**	**ΔH_m (J g^{-1})**	**X_C(%)**
0	62.8 ± 0.26	96.3 ± 0.62	12.5 ± 0.29	169.6 ± 0.66	34.5 ± 0.37	23.6 ± 0.75
2.5	61.7 ± 0.62	105.9 ± 0.56	30.4 ± 0.67	171.6 ± 0.59	35.2 ± 0.52	5.2 ± 0.98
5.0	61.6 ± 0.48	98.9 ± 0.56	24.9 ± 0.58	171.2 ± 0.49	36.9 ± 0.47	11.8 ± 0.94
7.5	59.9 ± 0.28	101.6 ± 0.45	26.8 ± 0.41	169.8 ± 0.82	35.0 ± 0.62	11.9 ± 0.86
10.0	59.4 ± 0.45	100.8 ± 0.36	26.6 ± 0.39	169.3 ± 0.47	38.2 ± 0.64	13.5 ± 0.85

Table 4.- Variation of the coefficient of linear thermal expansion (CLTE) below and above glass transition temperature (T_g), Vicat softening temperature (VST), and heat deflection temperature (HDT) of the injection-molded polylactide (PLA) parts varying the acrylated epoxidized soybean oil (AESO) content.

AESO content (wt%)	**CLTE below T_g (µm m^{-1} ºC^{-1})**	**CLTE above T_g (µm m^{-1} ºC^{-1})**	**VST (ºC)**	**HDT (ºC)**
0	94.4 ± 0.4	146.9 ± 0.4	56.3 ± 0.5	55.4 ± 1.6
2.5	89.6 ± 0.8	155.5 ± 1.2	56.0 ± 0.4	54.4 ± 0.4
5.0	90.6 ± 0.5	182.3 ± 7.2	55.8 ± 0.5	54.8 ± 0.6
7.5	90.7 ± 0.8	172.8 ± 2.4	54.0 ± 0.3	53.8 ± 0.4
10.0	92.4 ± 0.6	178.2 ± 3.8	53.6 ± 0.5	53.9 ± 0.7